



## Microstructure evolution of Al–Cu–Mg alloy during rapid cold punching and recrystallization annealing

Ze-yi HU<sup>1</sup>, Cai-he FAN<sup>1</sup>, Dong-sheng ZHENG<sup>1</sup>, Wen-liang LIU<sup>1</sup>, Xi-hong CHEN<sup>2</sup>

1. College of Metallurgy and Material Engineering, Hunan University of Technology, Zhuzhou 412007, China;
2. CRRC Zhuzhou Electric Locomotive Co., Ltd., Zhuzhou 412007, China

Received 31 October 2018; accepted 30 June 2019

**Abstract:** The microstructure evolution of spray formed and rapidly solidified Al–Cu–Mg alloy with fine grains during rapid cold punching and recrystallization annealing was investigated by transmission electron microscopy (TEM). The results show that the precipitates of fine-grained Al–Cu–Mg alloy during rapid cold punching and recrystallization annealing mainly consist of *S* phase and a small amount of coarse Al<sub>6</sub>Mn phase. With the increase of deformation passes, the density of precipitates increases, the size of precipitates decreases significantly, and the deformation and transition bands disappear gradually. In addition, the grains are refined and tend to be uniform. Defects introduced by rapid cold punching contribute to the precipitation and recrystallization, and promote nucleation and growth of *S* phase and recrystallization. Deformation and transition bands in the coarse grains transform into deformation-induced grain boundary during the deformation and recrystallization, which refine grains, obtain uniform nanocrystalline structure and promote homogeneous distribution of *S* phase.

**Key words:** Al–Cu–Mg alloy; microstructure evolution; precipitate; recrystallization; deformation band; rapid cold punching

### 1 Introduction

Al–Cu–Mg alloy has been widely applied to aerospace and military industries because of its advantage such as high strength, good formability and heat resistance [1,2]. Precipitation strengthening and grain refinement are the main strengthening and toughening methods. Under the conventional T6-like heat treatment, the main strengthening phase in Al–Cu–Mg alloy is *S* phase with low Cu/Mg ratios (Al<sub>2</sub>CuMg) and  $\theta'$  phase (Al<sub>2</sub>Cu) with high Cu/Mg ratios [3–6]. Deformation not only makes the material obtain good work hardening properties, but also introduces a large number of dislocations during the deformation. Aging process after deformation can release deformation stress, promote the dispersive nucleation and growth of precipitates, and even change the characteristics and precipitation sequence of precipitates [7–10]. STYLES et al [11] investigated the relationship between the decomposition sequence of supersaturated solid solution and the phase in Al–Cu–Mg alloy, and pointed out that the formation

time of *S* phase at higher temperature is much shorter than that at lower temperature. LI et al [12] investigated the effect of pre-deformation on the microstructure of high-purity Al–Cu–Mg alloy and found that the density of *S'* phase (Al<sub>2</sub>CuMg) increases while its size decreases with the increase of pre-deformation degree. YIN et al [13] studied the growth behavior of *S* precipitation phase particles within the grains of high strength Al–Cu–Mg alloy. It was reported that the structural units in the GPB region formed around *S* phase at higher aging temperature (above 180 °C) and hindered the growth of *S* phase along the width direction, resulting in the growth of *S* phase into columnar crystal. YANG et al [14] studied the effect of applied stress on the precipitation process of  $\theta'$  and *S* phases in Al–Cu–Mg alloy and found that applied stress prevented the precipitation of  $\theta'$  phase by changing the  $\theta'/S$  ratio during the competitive precipitation, thereby the precipitation of *S* phase was promoted. It can be seen that the microstructure evolution and phase structure characteristics of Al–Cu–Mg alloy have been studied under the conventional deformation and aging temperatures.

In the present work, the aluminum alloy cartridge

was prepared by rapid cold punching and recrystallization annealing, based on the spray formed Al–Cu–Mg alloy with fine grains. The precipitation phase, grain morphology and the evolution of deformation band during rapid cold punching and recrystallization annealing were studied. The interaction between precipitation phase and recrystallization, the formation mechanism of deformation band and its effect on grain refinement were discussed.

## 2 Experimental

Fine-grained Al–Cu–Mg alloy cylindrical billet was prepared by spray forming on a self-developed spray forming device SD380. The chemical composition of the alloy is shown in Table 1. The cylindrical billet was extruded into round bar with a diameter of 30 mm by a 1250T extruding machine at 723 K and the extrusion ratio was 15:1. Cylinder samples with 20 mm in length were cut from the bar by wire-cutting machine and then placed in a self-designed stamping die. After four passes of rapid cold punching and recrystallization annealing, the aluminum alloy cartridges were prepared. The schematic diagram of rapid cold punching is shown in Fig. 1. The process of rapid cold punching and recrystallization annealing is shown in Fig. 2. In the case of recrystallization annealing, the corresponding

**Table 1** Chemical composition of Al–Cu–Mg alloy (wt.%)

Cu	Mg	Mn	Si	Fe	Al
4.51	1.46	0.56	<0.05	<0.05	Bal.

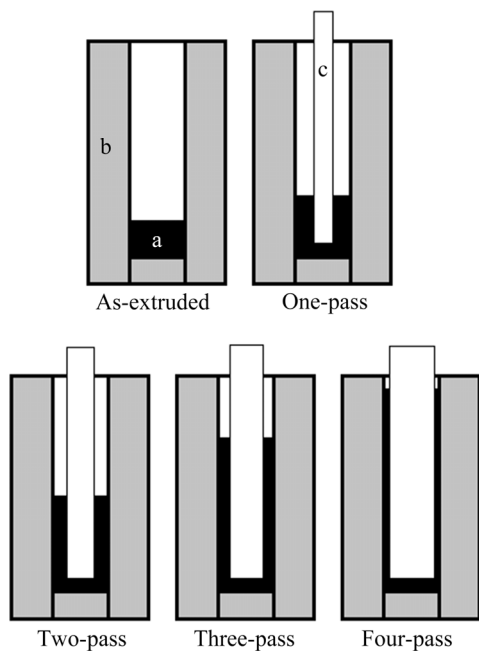


**Fig. 1** Schematic diagrams of rapid cold punching: a—Sample; b—Drawing die; c—Punch

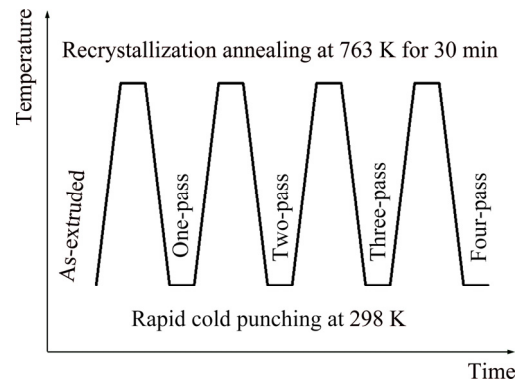


**Fig. 2** Process diagram of recrystallization annealing at 763 K for 30 min and rapid cold punching at 298 K

heating rate was 623 K/min. After holding for 30 min, the samples were cooled to room temperature and the next cold punching was performed. The process parameters of rapid cold punching are shown in Table 2.

The specimens were selected on the wall of cartridges for transmission electron microscopy (TEM) analysis. The preparation process of TEM specimens was as follows. The specimens were mechanically ground to 100  $\mu\text{m}$  before punching, and then finely ground to 70  $\mu\text{m}$ . After that, the specimens were twin jet electropolished in a mixed solution of 25% nitric acid and 75% methanol at 253 K using the voltage of 20 V. All specimens were washed in plasma cleaner Fishione, and their fine structures were observed in a Titan G2 60–300 transmission electron microscope. The electron microscopic parameters observed by high-angle annular dark-field scanning transmission electron microscopy (HAADF-STEM) were as follows. Acceleration voltage was 200 keV, half-convergence angle of electron beam was 10 mrad, inner half-angle of high-angle annular probe was 36 mrad, and beam spot diameter was 0.20 nm.

**Table 2** Process parameters of rapid cold punching

Punch	Diameter/mm	Velocity/( $\text{mm}\cdot\text{s}^{-1}$ )
One-pass	10	30
Two-pass	14	25
Three-pass	20	20
Four-pass	27	15

## 3 Results

### 3.1 Precipitation phase characteristics

The TEM images of the precipitation phases after recrystallization annealing of Al–Cu–Mg alloy specimens with different passes are shown in Fig. 3. EDS spectra of precipitation phase in Fig. 3(a) are shown in Fig. 4. The main precipitation phase of the alloy is *S*

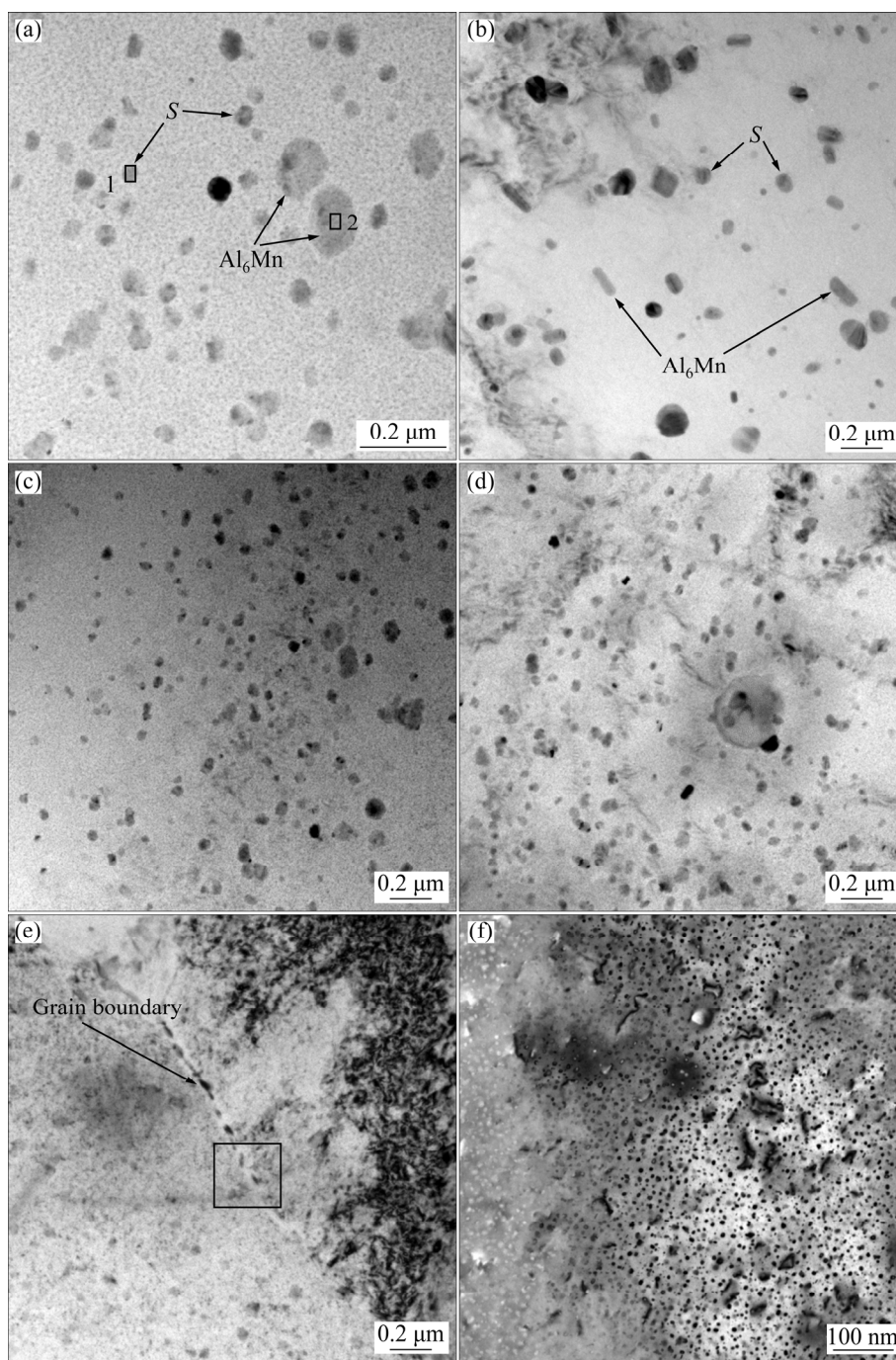


**Fig. 3** TEM images of precipitation phases in Al–Cu–Mg alloy specimens under different conditions: (a) As-extruded; (b) One-pass; (c) Two-pass; (d) Three-pass; (e, f) Four-pass

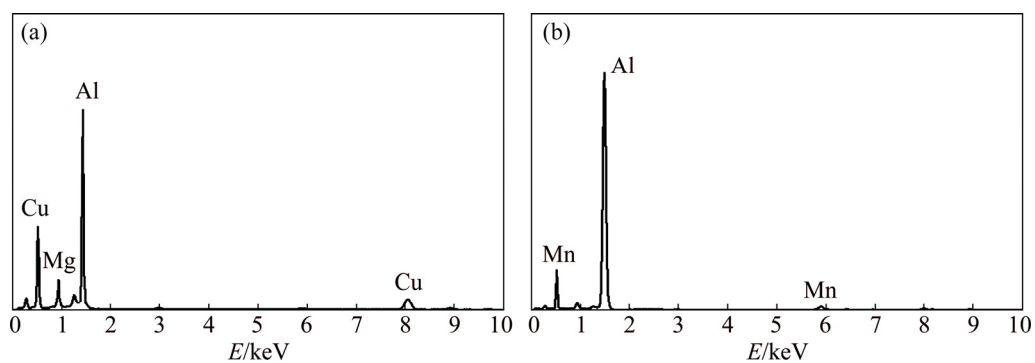


**Fig. 4** EDS spectra of precipitation phases in Al–Cu–Mg alloy specimens: (a) Position 1 in Fig. 3(a); (b) Position 2 in Fig. 3(a)

phase ( $\text{Al}_2\text{CuMg}$ ). Due to the addition of Mn, a small amount of coarse  $\text{Al}_6\text{Mn}$  phase can be observed. With the increase of deformation passes, the degree of deformation increases, the density of precipitation phase increases, the size decreases, and the precipitation phase tends to disperse. As a result of high deformation temperature of hot extruded alloy, the coarse  $\text{Al}_6\text{Mn}$  phase and  $S$  phase can be observed in the alloy (Fig. 3(a)). After rapid cold punching of one pass and recrystallization annealing, the size of precipitation phase significantly decreases, especially the  $\text{Al}_6\text{Mn}$  phase is refined obviously and its shape is elongated (Fig. 3(b)). After rapid cold punching of two or three passes and recrystallization annealing, the sizes of  $\text{Al}_6\text{Mn}$  and  $S$  phases decrease further, the amount of both phases increases, and the distribution of them in matrix tends to be more uniform. The elongated  $\text{Al}_6\text{Mn}$  phase decreases continuously, and the spherical  $\text{Al}_6\text{Mn}$  phase increases (Figs. 3(c) and (d)). Compared with the cold-punched specimens in the first three passes, the precipitation phases in the specimens through rapid cold punching of four passes and recrystallization annealing need to be observed clearly at a larger multiple. A larger multiple was used to observe the region near the grain boundary (the square area in Fig. 3(e)). It is found that the nano-sized precipitation phases are uniformly distributed in the matrix, and the size and morphology of the precipitation phases are basically the same (Fig. 3(f)).

### 3.2 Grain morphology

Figure 5 shows TEM micrographs of Al–Cu–Mg alloy specimens after rapid cold punching of different passes and recrystallization annealing. With the increase of deformation passes, both the deformation and recrystallization degrees of the specimens increase, the grain size becomes finer and finer, and the grain structure becomes more uniform. Incomplete recrystallization occurs in as-extruded alloy specimens annealed at 763 K for 30 min. Substructure with high dislocation density still exists near the recrystallization zone. The recrystallized grains are mainly in micron size, and a small number of recrystallized grains are found in the vicinity of coarse recrystallized grains (Fig. 5(a)). After rapid cold punching of one pass or two passes, the grain size of the specimens is obviously refined, the recrystallization degree increases and the dislocation density decreases, but it is still incomplete recrystallization. The recrystallized grains are mainly nanocrystalline, and some recrystallized grains grow to coarse grains (Figs. 5(b) and (c)). After rapid cold punching of three passes and recrystallization annealing, the specimens are fully recrystallized, and the microstructure becomes uniform. There are no coarse recrystallized grains, the recrystallized grains are all nanocrystalline, the average grain size is less than 100 nm, and the dislocation density is further reduced (Fig. 5(d)). When the specimens are subjected to rapid

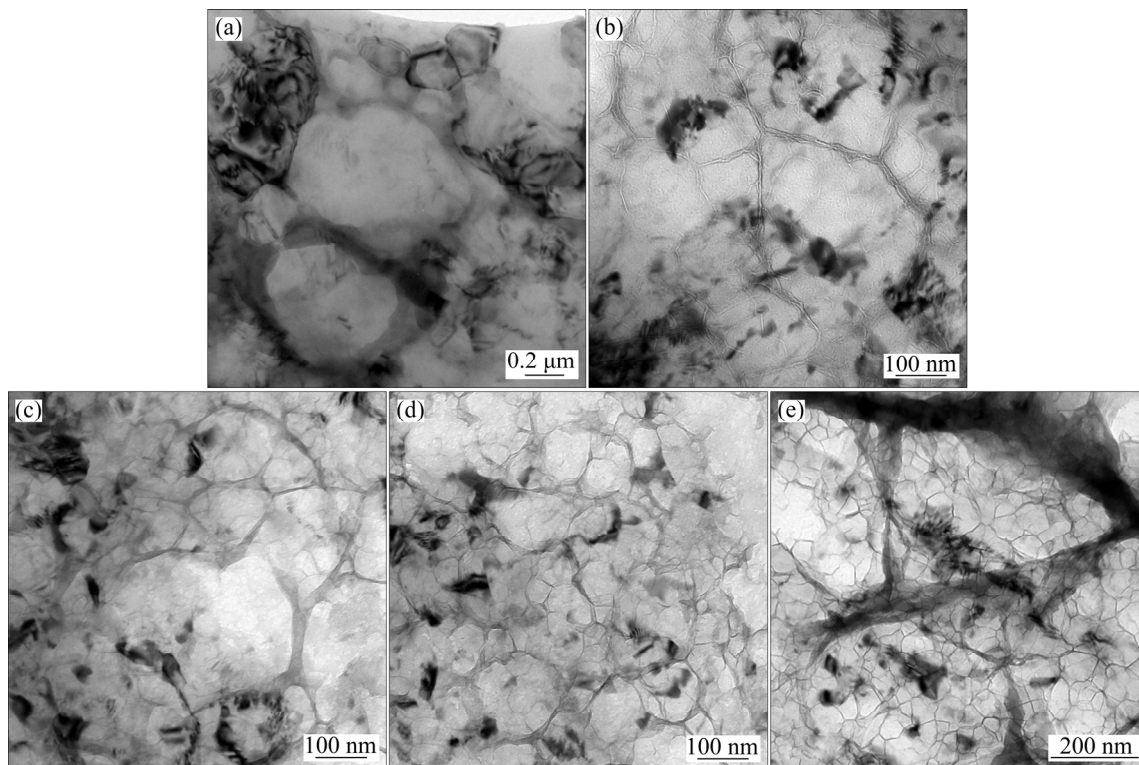


**Fig. 5** TEM images of Al–Cu–Mg alloy specimens under different conditions: (a) As-extruded; (b) One-pass; (c) Two-pass; (d) Three-pass; (e) Four-pass

cold punching of four passes and recrystallization annealing, the fully recrystallized structure is more uniform and the recrystallized grains are mainly equiaxed. Compared with the specimens through rapid cold punching of three passes, the grain size is further refined and the average grain size is less than 50 nm. Due to the increase of deformation degree and strain rate, the high dislocation density produced by cold punching still exists in the local region (Fig. 5(e)).

### 3.3 Deformation band and transition band

TEM images of deformation and transition bands in Al–Cu–Mg alloy specimens cold-punched with different passes are presented in Fig. 6. Deformation band with about 100 nm in width can be observed in coarse grains after single-pass rapid cold punching (Fig. 6(a)). When the rectangular region in Fig. 6(a) is further enlarged, the boundary of the deformation band with about 10 nm in thickness can be clearly observed, which is the transition band (Fig. 6(b)). The transition band is obviously narrowed after rapid cold punching deformation of two passes (Fig. 6(c)), and can hardly be observed in the case of rapid cold punching deformation of three passes (Fig. 6(d)).

## 4 Analysis and discussion

### 4.1 Interaction between precipitation phases and recrystallization

The dissolving sequence of Al–Cu–Mg alloy from high to low is generally GP region,  $S'$ (Al<sub>2</sub>CuMg),  $S$ (Al<sub>2</sub>CuMg). In this the work, GP zones,  $S'$  and  $S$  phases are found in Al–Cu–Mg alloy specimens after rapid cold punching of different passes and recrystallization annealing (Fig. 7). The GP region consists of Cu and Mg atom pairs enriched on {110} crystal plane [1] (Fig. 7(a)). These atom pairs strengthen the alloy by pinning dislocations. The  $S'$  phase, which is semi-coherent with the matrix, is mainly formed (Fig. 7(b)). The non-coherent equilibrium phase of granular  $S$  phase is formed undergoing four passes (Fig. 7(c)).

Previous studies have shown that the precipitation sequence of precipitates in Al–Cu–Mg alloy is related to heating temperature, deformation amount and grain size after deformation [15,16]. If the heating temperature can eliminate the high stress caused by strong deformation, the sequence is first transition phase, and then stable phase. If the heating temperature cannot eliminate the

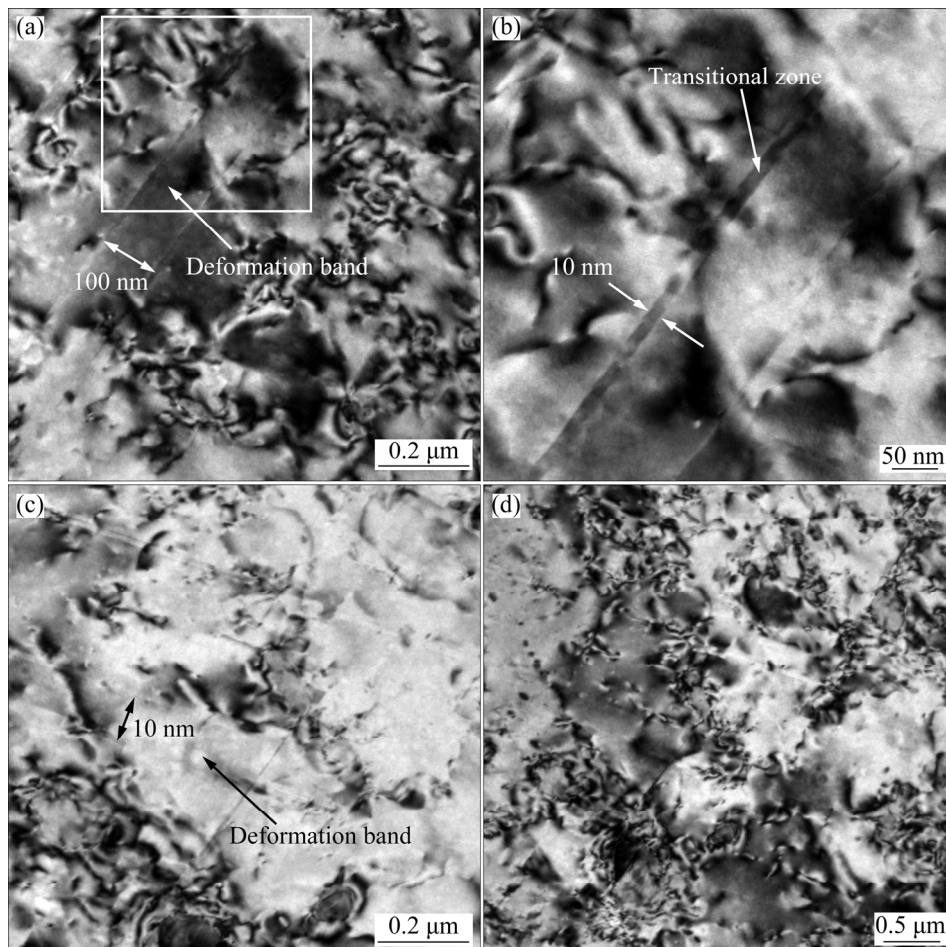


**Fig. 6** TEM images of deformation and transition bands in Al–Cu–Mg alloy specimens under different conditions: (a, b) One-pass; (c) Two-pass; (d) Three-pass

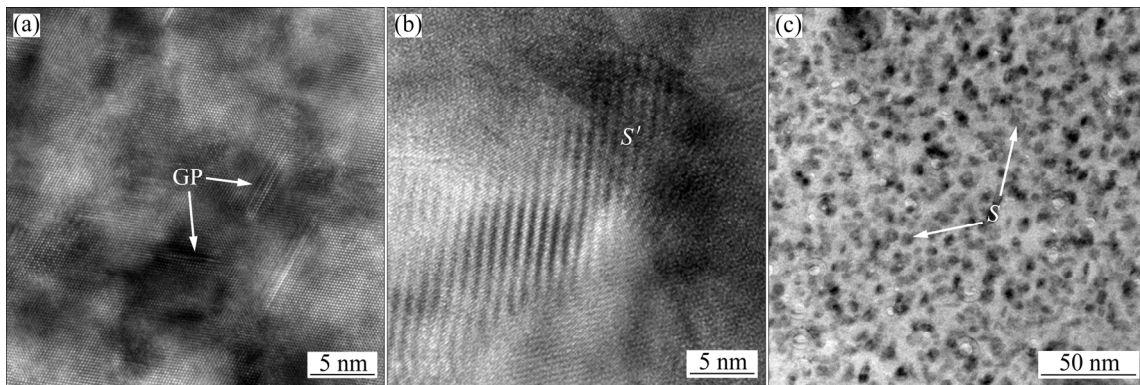


**Fig. 7** Phase morphologies of Al–Cu–Mg alloy specimens: (a) GP zones; (b)  $S'$  phase; (c)  $S$  phase

high stress, the grain size is ultra-fine. The transition phase is inhibited, and the stable phase is generated directly when reprecipitated. Based on the spray forming and rapid solidification technique, fine-grained Al–Cu–Mg alloy billet is prepared in this work. The Al–Cu–Mg alloy cartridge is prepared by multi-pass rapid cold punching, high temperature recrystallization annealing, rapid heating and slow cooling. With the increase of deformation passes, the density of precipitation phases increases, and their size decreases significantly (Fig. 3). A large number of  $S'$  phases can be observed in the specimen, which indicates that the main dissolving process during the forming of cartridge is first transition phase, and then the stable phase (Fig. 7). Meanwhile, the grain structure of the specimen tends to be homogeneous and the grains are refined to nanocrystalline (Fig. 5). Further analysis shows that the main reason for the above phenomena is the interaction between precipitates and recrystallization under the condition of rapid cold punching and high temperature recrystallization annealing [5,6]. Rapid cold punching significantly increases the dislocation density and becomes the most effective absorption source of vacancy, thus increasing the number of vacancies diffused to dislocation.  $S'$  phase nucleates preferentially at dislocation. The high density dislocation introduced by rapid cold punching provides the effective nucleation sites for  $S'$  phase, thereby the nucleation number of  $S'$  phase increases with the increase of rapid cold punching passes. It was reported that dissolving and recrystallization compete and interact with each other during the recrystallization annealing of supersaturated solid solution after deformation, and that the recrystallization process depends on the instantaneous equilibrium of the dissolving and recrystallization [17].

In this work, the defect introduced by rapid cold punching promotes dissolving and recrystallization nucleation, and the dissolving phase particles in turn pin the grain boundaries, thereby affecting the recrystallization nucleation and growth, so as to delay the

recrystallization. Further study shows that the rapid cold punching and recrystallization annealing process can obviously promote the recrystallization of spray-formed Al–Cu–Mg alloy and refine the microstructure of the specimens. The main reasons are as follows. Firstly, rapid heating in this experiment makes the dissolving particles too late to produce, reduces effectively the recrystallization temperature, and promotes the occurrence of recrystallization, leading to the precipitates formed during the subsequent recrystallization annealing to affect the recrystallization to proceed in the recrystallized grains. Obviously, the recrystallization annealing temperature is the critical factor affecting precipitation and recrystallized grains [18]. Secondly, there is a simple geometric relationship between the recrystallized grain size  $D_N$  and precipitation phase volume fraction  $f$  and particle radius  $r$  [18,19]:

$$D_N \approx 2rf^{-1/3} \quad (1)$$

As can be seen in Eq. (1), the larger the volume fraction of precipitation phase is, the smaller the radius of particles is, the finer the recrystallized grains are, which is consistent with the present result. Thirdly, the larger the deformation amount is, the larger the dislocation density is, thus increasing the deformation storage energy and the driving force of recrystallization. Meanwhile, the larger the deformation amount is, the greater the maximum orientation difference of the precipitation phase edge is. The larger orientation gradient is conducive to recrystallization nucleation, thus promoting the microstructure homogeneity and grain refinement of the alloy. Finally, certain amount of Mn is added to the alloy, resulting in intragranular segregation due to the grain boundary adsorption phenomenon of Mn. Elongated  $Al_6Mn$  phase is easily formed during the rapid cold punching and recrystallization annealing (Fig. 3(b)). The coarse  $Al_6Mn$  phase can further improve the deformation storage energy and increase the orientation difference at the edge of precipitates, thereby promoting the occurrence recrystallization.

#### 4.2 Formation mechanism of deformation band and its effect on grain refinement

During large deformation of high stacking fault energy aluminum alloy polycrystal, due to different crystallographic orientations of adjacent grains at grain boundaries, the deformation of each grain must be coordinated with the adjacent grains to maintain the continuity of polycrystal deformation. In this experiment, the specimens are divided into different orientation zones in coarse grains, i.e. deformation bands, because of the inhomogeneous stress of grains propagating to adjacent grains or the instability of grains during plastic deformation. Figure 8(a) shows the HRTEM image of the deformation and transition bands after rapid cold punching of one pass, and Fig. 8(b) shows schematic diagram of deformation and transition bands. As can be seen, region *B* is the original orientation region of the grain, and region *C* is the deformation band with different orientations from the original grain. Region *A* is the transition band with drastic change of orientation from region *B* to region *C*, and the orientation change across the transition band *A* has great gradient orientation. Studies indicate [1,20] that transition band *A* can be either a wide orientation region or a narrow orientation region, and can be transformed into the large angle grain boundary, i.e. deformation-induced grain boundary, under high strain rate deformation condition. The mechanism of transformation from transition band to deformation-induced grain boundary can effectively refine coarse grains and play an important role in obtaining uniform fine grain structure.

Studies [20,21] demonstrate that the occurrence of deformation band in high stacking fault energy polycrystal depends on the microstructure and deformation condition, and that the grain orientation determines the rotation of grains during deformation. The rotation of each part of coarse deformed grains varies greatly under the action of adjacent fine grains, resulting in deformation band or transition band. Lower deformation temperature will increase the inhomogeneity of deformation, so it helps to cause deformation band. In this experiment, the grain morphologies of Al–Cu–Mg alloy specimens under different states are observed (Fig. 5). It is found that the coarse grains exist in extruded and one pass or two passes cold-punched specimens to a certain extent. Therefore, the deformation and transition bands can be observed in the coarse grains (Figs. 6(a) and (b)). However, in the specimens after cold punching of three or four passes, the grain morphology tends to be consistent, the grain size is remarkably uniform and the deformation band is difficult to be observed in the specimens (Fig. 6(d)). It can be seen that the combination of rapid cold punching deformation and recrystallization annealing process, and the formation of

deformation and transition bands in the coarse grains under the process plays a decisive role in the grain refinement of the alloy, and there is a high correlation among them.

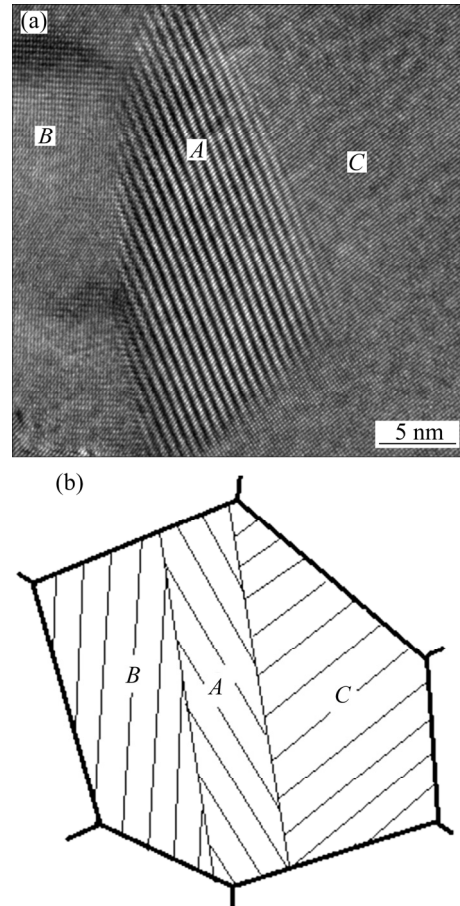


**Fig. 8** HRTEM image (a) and schematic diagram (b) of deformation and transition bands in Al–Cu–Mg alloy specimens undergoing one-pass deformation

## 5 Conclusions

(1) The precipitates of Al–Cu–Mg alloy during rapid cold punching and recrystallization annealing mainly consist of *S* phase and a small amount of coarse  $Al_6Mn$  phase. With the increase of deformation passes, the density of precipitates increases and the size decreases significantly.

(2) Rapid cold punching promotes the dissolving and recrystallization nucleation of the specimens by introducing defect, and contributes to the nucleation and growth of *S'* phase and recrystallization, and thus obtaining the nanocrystalline structure and dispersed *S* phase.

(3) Rapid cold punching favors the formation of deformation and transition bands in the coarse grains, and these bands transform into deformation-induced grain boundary during the deformation and recrystallization, thus effectively refining grains and obtaining uniform fine grains.

## References

- [1] WANG Zhu-tang, TIAN Rong-zhang. User manual for Al alloys and processing version [M]. 3rd ed. Changsha: Central South University Press, 2007. (in Chinese)
- [2] WILLIAMS J C, STARKE J E. Progress in structural materials for aerospace systems [J]. *Acta Materialia*, 2003, 51(19): 5775–5799.
- [3] WU Cui-lan, ZHOU Bin, NIU Feng-jiao, DUAN Shi-yun, GONG Xiang-peng, CHEN Jiang-hua. Deformation-induced  $\Omega$  phase precipitation strengthening of AlCuMg alloy with high Cu/Mg atomic ratio [J]. *Journal of Hunan University*, 2018, 45(6): 1–10. (in Chinese)
- [4] GAZIZOV M, KAIBYSHEV R. Effect of pre-straining on the aging behavior and mechanical properties of an Al–Cu–Mg–Ag alloy [J]. *Materials Science and Engineering A*, 2015, 625(14): 119–130.
- [5] ZHAO Y L, YANG Z Q, ZHANG Z. Double-peak age strengthening of cold-worked 2024 aluminum alloy [J]. *Acta Materialia*, 2013, 61(5): 1624–1638.
- [6] ZUIKO I S, GAZIZOV M R, KAIBYSHEV R O. Effect of thermomechanical treatment on the microstructure, phase composition, and mechanical properties of Al–Cu–Mn–Mg–Zr alloy [J]. *Physics of Metals and Metallography*, 2016, 117(9): 906–919.
- [7] XU Fu-shun, ZHANG Jin, DENG Yun-lai, ZHANG Xin-ming. Effect of snake rolling on strength, toughness and microstructure of Al–Cu–Mg alloy plate [J]. *The Chinese Journal of Nonferrous Metals*, 2017, 27(10): 2005–2011. (in Chinese)
- [8] MIRZAEI M, ROSHAN M R, JENABALI JAHROMI S A. Microstructure and mechanical properties relation in cold rolled Al2024 alloy determined by X-ray line profile analysis [J]. *Materials Science and Engineering A*, 2015, 620: 44–49.
- [9] AN Li-hui, CAI Yang, LIU Wei, YUAN Shi-jian, ZHU Shi-qiang, MENG Fan-cheng. Effect of pre-deformation on microstructure and mechanical properties of 2219 aluminum alloy sheet by thermomechanical treatment [J]. *Transactions of Nonferrous Metals Society of China*, 2012, 22(2): 370–375.
- [10] LI Zhou-bing, SHEN Jian, LEI Wen-ping, YAN Liang-ming, LI Jun-peng, MAO Bai-ping. Effects of prestretching on precipitated phase and mechanical properties of Al–Cu–Mg–Ag alloy [J]. *The Chinese Journal of Nonferrous Metals*, 2010, 20(8): 1508–1512. (in Chinese)
- [11] STYLES M J, MARCEAU R K W, BASTOW T J, BRAND H E A, GIBSON M A, HUTCHINSON C R. The competition between metastable and equilibrium  $S(\text{Al}_2\text{CuMg})$  phase during the decomposition of Al–Cu–Mg alloys [J]. *Acta Materialia*, 2015, 98(1): 64–80.
- [12] LI Hui-zhong, LIU Ruo-mei, LIANG Xiao-peng, DENG Min, LIAO Hui-juan, HUANG Lan. Effect of pre-deformation on microstructures and mechanical properties of high purity Al–Cu–Mg alloy [J]. *Transactions of Nonferrous Metals Society of China*, 2016, 26(6): 1482–1490.
- [13] YIN Mei-jie, CHEN Jiang-hua, LIU Chun-hui. Effect of interrupted ageing on mechanical property and microstructure of AA2024 alloy [J]. *The Chinese Journal of Nonferrous Metals*, 2015, 25(12): 3271–3281. (in Chinese)
- [14] YANG Pei-yong, ZHENG Zi-qia, XU Fu-shun, LI Shi-chen, LI Jian, ZHOU Ming. Effect of external stress on kinetics of precipitation and morphologies of precipitates in Al–Cu–Mg alloy with high Cu/Mg ratio [J]. *Rare Metals*, 2006, 30(3): 324–328.
- [15] ZHAO Yun-long, YANG Zhi-qing, ZHANG Zhen, SU Guo-yue, MA Xiu-liang. Double-peak age strengthening of cold-worked 2024 aluminum alloy [J]. *Acta Materialia*, 2013, 61(6): 1624–1638.
- [16] MOGHANAKI S K, KAZEMINEZHAD M. Effects of non-isothermal annealing on microstructure and mechanical properties of severely deformed 2024 aluminum alloy [J]. *Transactions of Nonferrous Metals Society of China*, 2017, 27(1): 1–9.
- [17] ZHOU Ze-peng, ZHANG Jing, DENG Yun-lai, ZHANG Xin-ming. Creep forming heat treatment technology of Al–Cu–Mg alloy [J]. *The Chinese Journal of Nonferrous Metals*, 2017, 27(8): 1607–1614.
- [18] PONGE D, GOTTSTEIN G. Necklace formation during dynamic recrystallization: Mechanisms and impact on flow behavior [J]. *Acta Materialia*, 1998, 46(1): 69–80.
- [19] HUMPHREYS F J. A unified theory of recovery, recrystallization and grain growth, based on the stability and growth of cellular microstructures—I [J]. *Acta Materialia*, 1997, 45(10): 4231–4240.
- [20] ZIEGENBEIN A, HAHNER P, NEUHAUSER H. Correlation of temporal instabilities and spatial localization during Portevin-Le Chatelier deformation of Cu–10at.%Al and Cu–15at.%Al [J]. *Computational Materials Science*, 2000, 19(3): 27–34.
- [21] JIANG Hui-feng, ZHANG Qing-chuan, JIANG Zhen-yu, ZHAO Si-min, CHEN Zhong-jia, WU Xiao-ping. Investigation on the Portevin-Le Chatelier deformation bands in Al–Cu alloys [J]. *Journal of Experimental Mechanics*, 2004, 19(4): 430–436.

## Al–Cu–Mg 合金在快速冷冲及再结晶退火过程中的显微组织演变

胡泽艺<sup>1</sup>, 范才河<sup>1</sup>, 郑东升<sup>1</sup>, 刘文良<sup>1</sup>, 陈喜红<sup>2</sup>

1. 湖南工业大学 冶金与材料工程学院, 株洲 412007; 2. 中国中车株洲电力机车有限公司, 株洲 412007

**摘要:** 采用透射电镜技术(TEM)系统研究喷射成形快速凝固细晶 Al–Cu–Mg 合金在快速冷冲及再结晶退火工艺过程中的显微组织演变。结果表明: 细晶 Al–Cu–Mg 合金在快速冷冲及再结晶退火过程中的析出相主要为  $S$  相, 还有少量较粗的  $\text{Al}_6\text{Mn}$  相; 随着变形道次的增加, 析出相的密度不断增大、尺寸显著减小, 形变带和过渡带逐渐消失, 晶粒组织不断细化并趋于均匀。快速冷冲引入的缺陷有助于 Al–Cu–Mg 合金脱溶和再结晶形核, 促进  $S$  相和再结晶的形核与长大。较粗晶粒中的形变带及过渡带在形变和再结晶过程中转变为形变诱发晶界, 从而细化晶粒、获得均匀纳米晶组织和促进  $S$  相弥散分布。

**关键词:** Al–Cu–Mg 合金; 显微组织演变; 析出相; 再结晶; 形变带; 快速冷冲

(Edited by Wei-ping CHEN)